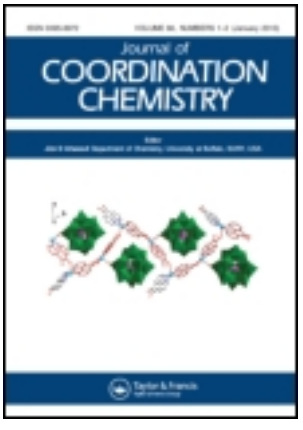

Journal of Coordination Chemistry
Publication details, including instructions for authors and subscription information:
http://www.tandfonline.com/loi/gcoo20

Examining the binding mechanism of 3,4-dihydro-3-(2-oxo-2-phenylethylidene)-quinoxalin-2(1H)-one and its fragments to Cu^{2+}

Efrat Korin [a], Beny Cohen [a], Yong-Dong Liu [b], Cheng-Chu Zeng [b], Alexander I. Shames [c] & James Y. Becker [a]

[a] Department of Chemistry, Ben-Gurion University of the Negev, Beer Sheva, Israel

[b] College of Life Science & Bioengineering, Beijing University of Technology, Beijing, China

[c] Department of Physics, Ben-Gurion University of the Negev, Beer Sheva, Israel

Accepted author version posted online: 08 May 2013.Published online: 14 Jun 2013.

To cite this article: Efrat Korin, Beny Cohen, Yong-Dong Liu, Cheng-Chu Zeng, Alexander I. Shames & James Y. Becker (2013) Examining the binding mechanism of 3,4-dihydro-3-(2-oxo-2-phenylethylidene)-quinoxalin-2(1H)-one and its fragments to Cu^{2+}, Journal of Coordination Chemistry, 66:13, 2351-2366, DOI: 10.1080/00958972.2013.803535

To link to this article: http://dx.doi.org/10.1080/00958972.2013.803535

Journal of Coordination Chemistry, 2013
Vol. 66, No. 13, 2351–2366, http://dx.doi.org/10.1080/00958972.2013.803535

Examining the binding mechanism of 3,4-dihydro-3-(2-oxo-2-phenylethylidene)-quinoxalin-2(1H)-one and its fragments to Cu^{2+}

EFRAT KORIN†, BENY COHEN*†, YONG-DONG LIU‡, CHENG-CHU ZENG*‡, ALEXANDER I. SHAMES§ and JAMES Y. BECKER*†

†Department of Chemistry, Ben-Gurion University of the Negev, Beer Sheva, Israel
‡College of Life Science & Bioengineering, Beijing University of Technology, Beijing, China
§Department of Physics, Ben-Gurion University of the Negev, Beer Sheva, Israel

(*Received 11 December 2012; in final form 21 March 2013*)

The structure and stoichiometries of the complexes that could be formed between Cu^{2+} and 3,4-dihydro-3-(2-oxo-2-phenylethylidene)-quinoxalin-2(1H)-one (**1**) were investigated by various spectral techniques such as IR, fluorescence, UV–vis and electron paramagnetic resonance (EPR). The results suggest that initially 3 : 1 and 2 : 1 (**1**/Cu^{2+}) complexes are formed at low Cu^{2+} concentration and upon adding more Cu^{2+}, 1 : 1 (preferred) and 1 : 2 complexes are generated. Since **1** possesses two possible binding sites, further exploration was done by testing the binding ability of Cu^{2+} to fragments of **1**, namely β-enaminoketone derivatives (**2–3**) and quinoxaline-2-one (**4**), and by executing calculations of thermodynamic parameters of the reaction between **1** and Cu^{2+} in ethanol, optimized geometries of the possible complexes, and estimation of stability constants at various stoichiometries. Consequently, a step-by-step binding mechanism is suggested for formation of various complexes between **1** and Cu^{2+}.

Keywords: Quinoxalinone derivatives; Chelate; Cu^{2+} binding; N,O; Ligands; Stability constants

1. Introduction

Tremendous efforts have been devoted to development of chemosensors capable of selective and sensitive determination of specific heavy metal cations, such as Zn^{2+}, Cu^{2+}, and Co^{2+} [1–4]. One heavy metal that has received considerable attention is copper. It is an essential trace element that is required for various human physiological processes including electron transport and enzymatic catalysis. On the other hand, elevated levels of Cu^{2+} could become toxic. Also, it is generally accepted that copper is involved in a number of diseases such as cancer and neurodegenerative diseases (like Alzheimer and Parkinson) [5–8]. Thus, the detection and quantification of this metal ion has important environmental, biological, and medical applications. Accordingly various chemosensors for Cu^{2+} ion have been reported, usually containing an ionophore having 'N' and 'O' donors [9–22].

*Corresponding authors. Email: becker@bgu.ac.il (J.Y. Becker); bcohen@bgu.ac.il (B. Cohen); zengcc@bjut.edu.cn (C.-C. Zeng)

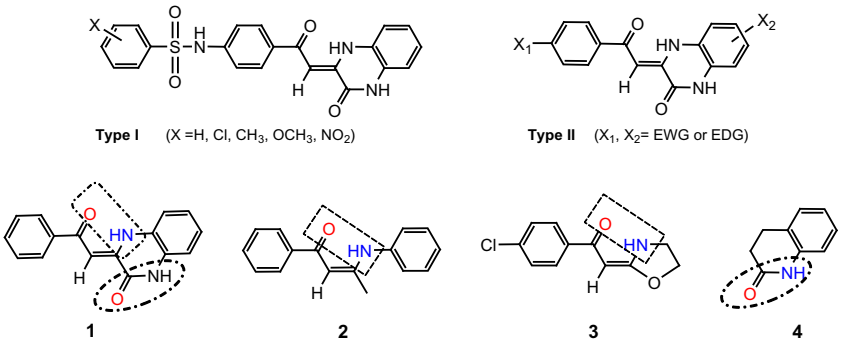

Scheme 1. Chemical structures of Types I and II derivatives, the building block 3,4-dihydro-3-(2-oxo-2-phenylethylidene)-quinoxalin-2(1H)-one (**1**), and its fragments **2**–**4**. The location of the potential binding site in each structure is marked by dashed lines.

Previously we reported on a series of organic fluorescent compounds based on sulfonamido derivatives of 3,4-dihydro-3-(2-oxo-2-phenylethylidene)-quinoxalin-2(1H)-one (named Type I in scheme 1) as potential chemosensors for Cu^{2+} [23]. In ethanol, these compounds display a highly selective response towards Cu^{2+} causing a red shift in the UV–vis absorption spectra and selective fluorescence quenching behavior. Other metal ions such as Zn^{2+}, Mg^{2+}, Co^{2+}, Ni^{2+}, Mn^{2+}, Ca^{2+} and Ag^{+} did not exhibit any spectral response. The UV–vis and fluorescence spectral response that were observed in the presence of Cu^{2+} were attributed to formation of a reversible metal–ligand complex. Recently, a new series (Type II, scheme 1) of fluorogenic chelating reagents based on the building block of Type I derivatives, having different substituents at different positions, was synthesized. The effect of the nature and position of the substituents on the spectral properties of the free ligands and their response towards Cu^{2+} in ethanol were studied and reported [24]. According to the fluorescence measurements the recognition selectivity towards Cu^{2+} could be finely tuned by the position and nature of the substituent, where either electron-donating group attached to the quinoxaline-2-one or electron-withdrawing group attached to the phenyl ring can enhance the response selectivity toward Cu^{2+}.

The present study aims towards better understanding of the binding mechanism between Cu^{2+} and the chelating agent **1** in ethanol. Furthermore, in order to determine which of the two possible binding sites in **1** is the actual one for binding Cu^{2+}, other ligands (**2**–**4**), fragments of **1** (each contains only one of the suspected binding sites), were synthesized and examined spectroscopically.

2. Experimental

2.1. *General*

Absorption spectra were acquired with an Agilent (HP) 8453 UV–vis Diode Array spectrophotometer (single beam) with wavelength accuracy $< \pm 0.5$ nm and photometric accuracy $< \pm 0.005$ AU. Fluorescence excitation spectra were acquired with a JASCO spectroflourimeter (Model FP-6500, Jasco Intern. Co., Japan) equipped with a 150 W xenon lamp. Both excitation and emission slit widths were 3 nm. ESI-MS analyses were performed by using a LTQ Orbitrap XL mass spectrophotometer (Thermo Scientific,

Germany and USA). Also, mass spectra were obtained with MALDI-TOF spectrometer reflex IV (Bruker Daltonic, Germany). FTIR spectra were recorded from 400–4000 cm^{-1} with a JASCO FTIR-615 spectrometer by using KBr pellets. Electron paramagnetic resonance (EPR) spectra were recorded using Bruker EMX-220 X-band ($\nu = 9.4$ GHz) EPR spectrometer. All measurements were conducted at 25 °C. In the UV–vis measurements, absolute ethanol was used.

2.2. *Computation methods*

2.2.1. Geometry optimization and thermodynamic parameters. Electron correlation effects were included employing DFT methods which have been widely proclaimed as a practical and effective computational tool, especially for organometallic compounds. Hybrid Hartree-Fock/Density functional calculations were performed by using B3LYP (Becke's three-parameter nonlocal exchange functional [25] with the correlation functional of Lee, Yang, and Parr [26]) in conjunction with the LanL2dz basis set for Cu and 6–311 + G(d,p) basis set for other atoms. The solvent effects were considered with the polarizable continuum model [27] and United Atom Kohn-Sham (UAKS) cavity was selected in the model. The geometries of all structures were fully optimized. Unless otherwise noted, all discussions in the following sections are based on the energy data obtained in ethanol solution. All calculations were performed with the Gaussian 03 program package [28].

2.2.2. Calculation of stability constants. ReactLab^{TM} Equilibria software is based on least square fitting of non-linear parameters (rate and equilibrium constants) using a modified Marquardt–Levenberg algorithm.

2.3. *Synthesis and characterization of ligands 1–4*

2.3.1. Synthesis of (Z)-3-(2-Oxo-2-phenylethylidene)-3,4-dihydroquinoxalin-2-one (1) [24]. A mixture of (*Z*)-2-hydroxy-4-oxo-4-phenylbut-2-enoic acid (1 mM), *o*-phenylenediamine (1.2 mM) and 60 mL mixed solvent ($V_{DMF} : V_{H_2O} = 1 : 1$) was refluxed under stirring for 2–4 h while TLC monitoring the reaction. After the completion of reaction the mixture was cooled to room temperature and a large amount of water was added. The desired product was collected by filtration, washed with water, and then with ether to remove the residual diamine. High quality 3,4-dihydroquinoxalin-2-one derivative **1** was obtained after recrystallization from DMF. Yield: 75%; m.p.: 277–278 °C; ^{1}H NMR (400 MHz, DMSO-d_6): δ 6.82 (s, 1H), 7.12–7.15 (m, 3H), 7.53 (s, 1H,), 7.50∼7.60 (m, 3H), 7.97–7.99 (m, 2H), 12.04 (s, 1H), 13.67 (s, 1H); ^{13}C NMR (100 MHz, DMSO-d_6): δ 89.6, 115.8, 117.1, 124.2, 124.5, 124.6, 127.2, 127.5, 129.2, 132.4, 139.1, 146.1, 156.2, 188.9; IR (KBr): ν 3437, 1628, 1376, 1264 cm^{-1}; ESI-MS: *m/z* 262.5 ($M^+ - 1$).

2.3.2. Synthesis of (Z)-1-phenyl-3-(phenylamino)but-2-en-1-one (2) [29, 30]. To a stirred solution of 3 mM of aniline and 3 mM of 1-phenylbutane-1,3-dione in 3 mL of EtOH, 5 mol% of CAN was added. The mixture was stirred at room temperature for 2 h. After completion of the reaction, the mixture was dissolved in CH_2Cl_2, washed with H_2O, dried, and evaporated. Analytically pure yellow solid **2** was obtained by rapid column chromatography on Et_3N pretreated silica gel, eluting with PE–EtOAc mixtures. Yield: 84%; m.p.: 109–111 °C; ^{1}H NMR (400 MHz, $CDCl_3$): δ 2.16 (s, 3H), 5.92 (s, 1H), 7.15–7.23 (m, 3H), 7.37–7.50 (m, 5H), 7.91–7.94 (m, 2H), 13.11 (br s, 1H, NH); ^{13}C NM

(100 MHz, $CDCl_3$): δ 20.5, 94.1, 124.8, 125.9, 127.1, 128.3, 129.0, 130.9, 138.5, 140.1, 162.1, 188.8.

2.3.3. Synthesis of (E)-1-(4-chlorophenyl)-2-(oxazolidin-2-ylidene)ethanone (3) [31]. To a solution of 3.7 g (60 mM) 2-aminoethanol in 30 mL dried tetrahydrofuran (THF) was added 1.4 g (36 mM) of sodium. The reaction mixture was stirred at room temperature. After the disappearance of sodium, 11.92 g (50 mM) of 1-(4-chlorophenyl)-3,3-bis(methylthio)prop-2-en-1-one in 100 mL THF was added. The reaction mixture was heated to reflux for 10 h. After cooling to room temperature, the whole mixture was poured into 100 mL of water and extracted with chloroform (30 mL × 3). The organic phase was dried with anhydrous sodium sulfate and after removal of the solvent, the crude product was recrystallized from methanol to give a white solid. Yield: 58%; m.p.: 197–199 °C. ^{1}H NMR (400 MHz, DMSO-d_6) δ 3.77 (t, 2H, J = 7.2 Hz), 4.44–4.48 (m, 2H), 5.49 (s, 1H), 7.21 (d, 2H, J = 8.0 Hz), 7.72 (d, 2H, J = 8.0 Hz), 9.78 (s, br, 1H, NH).

2.3.4. Synthesis of 3,4-dihydroquinolin-2(1H)-one (4) [32, 33]. Aniline (0.93 g, 10 mM) was dissolved in 5 mL of acetone. 3-Chloropropanoyl chloride (0.52 mL, 5 mM) was added dropwise at 0 °C. The addition lasted for about 30 min. Then stirring was continued for 4 h at room temperature. After completion of the reaction, 4 mL of HCl (5%) was added. The formed precipitate was filtered, washed with 5% HCl and water. The intermediate 3-chloro-*N*-phenylpropanamine was finally obtained in 93% yield.

A mixture of 3-chloro-*N*-phenylpropanamine (530 mg, 2.9 mM) and $AlCl_3$ (1.15 g, 8.7 mM) was heated to 150 °C and kept at the temperature for 4 h. Then the reaction mixture was poured into 100 mL of ice-water. The formed solid was filtered, washed twice, and dried to obtain 3,4-dihydroquinolin-2(1H)-one (**4**) in 90% yield. White solid was obtained after recrystallization from methanol. m.p.: 162–163 °C; ^{1}H NMR (400 MHz, $CDCl_3$): δ 2.65 (t, J = 7.2 Hz, 2H), 2.97 (t, J = 7.2 Hz, 2H), 6.87 (d, J = 7.6 Hz, 1H), 6.99 (t, J = 7.2 Hz, 1H), 7.25–7.07 (m, 2H), 9.47 (s, br, 1H, NH); ^{13}C NMR ($CDCl_3$, 100 MHz) δ 25.3, 30.4, 115.6, 123.1, 123.5, 127.5, 127.9, 137.4, 172.4.

2.4. *Reagents and general procedure*

Solutions of metal ions of perchlorate salts of Cu^{2+}, Zn^{2+}, Mn^{2+}, Na^+, and nitrate salts of Mg^{2+}, Co^{2+}, Ni^{2+}, Ca^{2+}, and Ag^+ (caution: perchlorate salts are potentially explosive) were prepared. All reagents were purchased from commercial suppliers (Aldrich and Merck). Ethanol was purchased from Bio Lab., Israel. All chemicals and solvents used in this work were of analytical grade, and used without further purification. However, in HR-ESI-MS measurements, HPLC grade solvents were used. In FTIR, KBr powder (Merck for IR spectroscopy) was used to prepare the pellets after drying the salt overnight in an oven at 100 °C.

2.4.1. Preparation of sample solutions for the evaluation of the photophysical properties of the ligands and their response to metal cations. Stock solutions of ligands **1**, **2** and **3** (2.4×10^{-5} M), and **4** (3×10^{-5} M) in ethanol were prepared. To

evaluate their selectivity to specific metal cation, stock solutions of 0.12 M of Cu^{2+}, Zn^{2+}, Mg^{2+}, Co^{2+}, Ni^{2+}, Mn^{2+}, Ca^{2+}, and Ag^{+} were also prepared in ethanol. Test samples were prepared by adding 80 μL of one of the mentioned metal stock solution to 4 mL of a ligand stock solution.

2.4.2. Preparation of stock solutions and samples for 1 titration experiments with Cu^{2+}. Stock solutions of 1×10^{-3} M of $Cu(ClO_4)_2$ in ethanol was prepared. 0–260 μL of $Cu(ClO_4)_2$ solution was added to 5 mL of **1** (2.4×10^{-5} M). In general, the spectrophotometric titration data were collected 2 h after addition of Cu^{2+}. The results obtained in a short time frame (minutes) (figure S11) were analyzed by using ReactLab™ Equilibria program.

2.4.3. EPR titration measurements of the ligands with Cu^{2+}. A stock solution of 4×10^{-2} M $Cu(ClO_4)_2$ was in ethanol. Stock solutions of 2 mM of **1**, **2**, and **4** were prepared in ethanol. Samples for the titration measurements of **1** were prepared by adding 15–500 μL of $Cu(ClO_4)_2$ to 2 mL of **1** (2 mM). Samples for the titration measurements of **2** were prepared by adding 15–200 μL of $Cu(ClO_4)_2$ solution to 2 mL of **2** (2 mM). Samples for the titration measurements of **4** were prepared by adding 15–125 μL of $Cu(ClO_4)_2$ solution to 2 mL of **4** (2 mM).

2.4.4. Preparation of samples for FTIR measurements of the ligands and their Cu^{2+} complexes. FTIR spectra of **1**, **2**, **3**, and **4** were prepared by the standard KBr pellet technique. To assess the binding ability of these ligands to Cu^{2+} solutions of the ligand (2 mM) with ~1 equiv. of Cu^{2+} perchlorate were prepared in ethanol and then left for air-drying. Then samples were prepared from the dried powder as KBr pellets.

2.4.5. Preparation of samples for HR-ESI-MS and MALDI-TOF measurements. Stock solutions (1 mM) of **2** and **4** were prepared in absolute ethanol (dehydrated, HPLC grade). A solution of $Cu(ClO_4)_2$ in ethanol (0.1 M) was also prepared. Samples were prepared by adding 1 equiv. of Cu^{2+} to 2 mL of the ligand (**2** or **4**) in ethanol. Then the samples were diluted with ethanol to a final concentration of 10 μM before they were analyzed by HR-ESI-MS. For MALDI-TOF-MS measurements, 2,5-dihydroxybenzoic acid matrix (DHB) (10 mg mL^{-1} in 90 : 10 v/v of deionized water/ethanol) was used. The MALDI sample was prepared first by mixing 10 μL of ethanol with 10 μL of the sample containing **2** in the presence of 1 equiv. of Cu^{2+} and then by adding 10 μL of the matrix. Afterwards 1 μL of the final sample was loaded onto a target plate and allowed to dry at room temperature before analyzed.

3. Results and discussion

3.1. *Investigating the binding mechanism of 1 towards Cu^{2+} in ethanol*

In order to understand the binding mechanism of Cu^{2+} to the ligand, various spectroscopic techniques and procedures (e.g. spectrophotometric and flourimetric titration, EPR titration,

FTIR, synthesis of fragments **2–4**, computations of optimized geometries, stability constants, and stoichiometries) have been applied to pursue this goal.

3.1.1. Titration experiments and binding stoichiometries for 1. At first, spectrophotometric and fluorimeteric titration experiments have been carried out in ethanol in order to study the binding properties of **1** towards Cu^{2+}. The results obtained are presented in figure 1. As can be observed from the UV–vis titration measurements (figure 1(a)), the three absorptions of free **1** at ~393, 415, and 438 nm were shifted to longer wavelengths (red shifts) along with a continuous decrease in intensity of the first two bands around 393 and 415 nm and simultaneous increase in the intensity of the band at 463 nm with increasing concentration of Cu^{2+}. At the same time, the fluorescence emission intensity of **1** ($\lambda_{ex} = 438$ nm) was gradually quenched as the Cu^{2+} concentration increased, with no significant change in the position of the emission maxima (figure 1(b)).

Based on the above measurements, the spectrophotometric and fluorimetric titration profiles of **1** with Cu^{2+} in ethanol are shown in figure 2. The binding stoichiometry appears to depend on the total amount of Cu^{2+} added to the ligand solution. Qualitatively,

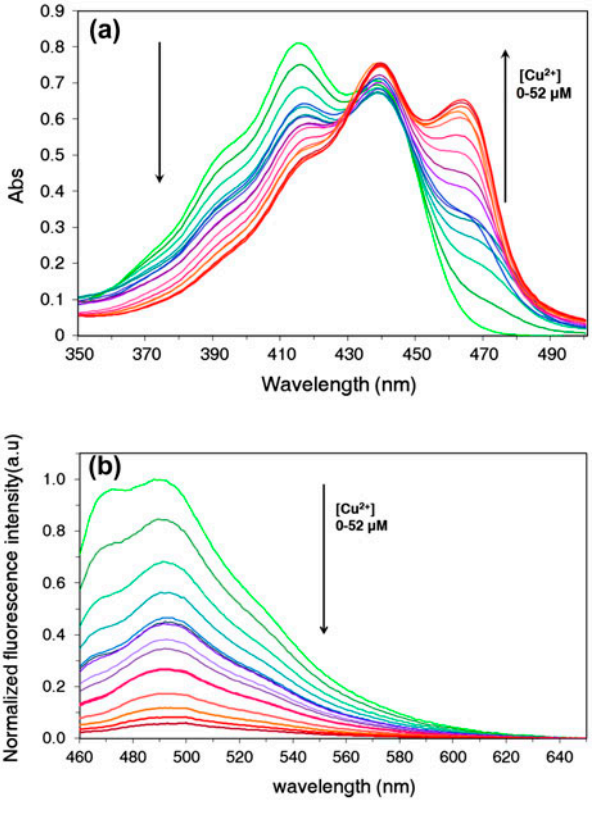

Figure 1. Spectral changes of **1** (24 μM) upon addition of increasing amounts of Cu^{2+} in ethanol (0, 2.4, 4.8, 7.2, 9.6, 12, 14.4, 16.8, 19.2, 24, 28, 32, 36, 48, 52 μM). (a) Spectral changes observed in the UV–vis absorption spectra. (b) Spectral changes observed in the fluorescence spectra during the titration experiments ($\lambda_{ex} = 438$ nm). Arrows indicate the absorbences that increased (up) and decreased (down) during the titration experiments.

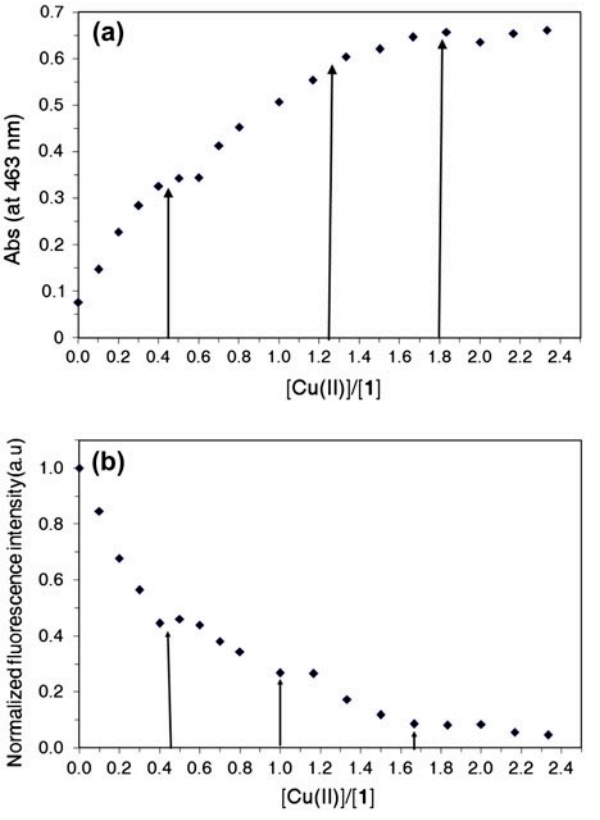

Figure 2. (a) A plot of absorption for the titration of **1** with Cu^{2+} in ethanol vs. $[Cu^{2+}]/[\mathbf{1}]$ ratio at 463 nm; (b) titration profile of the normalized fluorescence intensity ($\lambda_{ex} = 438$ nm, $\lambda_{em} = 474$ nm) for **1** in ethanol vs. $[Cu^{2+}]/[\mathbf{1}]$ ratio.

as indicated by arrows, it seems that at low concentrations of Cu^{2+} (<0.5 equiv.), a 2 : 1 complex is formed between **1** and Cu^{2+}, whereas at larger amounts of Cu^{2+} (1 equiv. or more), 1 : 1 and 1 : 2 complexes could be formed. Such a behavior is not unusual, since similar changes in ligand to metal stoichiometry at different concentrations of Cu^{2+} were observed in the formation of various chelates of tetradentate Schiff bases [34].

Furthermore, EPR titration measurements of **1** with Cu^{2+} also confirm the existence of two types of complexes between **1** and Cu^{2+} (figure 3(a)). At first, when 0.15 equiv. of Cu^{2+} was added to the ethanolic solution (in the absence of the ligand) no signal was recorded, but when the same amount of Cu^{2+} was added to **1**, an EPR signal corresponding to the 2 : 1 complex between **1** and Cu^{2+} (with $A_{iso} = 5.3(1)$ mT and $g_{iso} = 2.128(1)$) was observed. Moreover, as the amount of Cu^{2+} was increased the EPR spectrum slowly changed its shape by increasing the intensities of the signals around 316 and 320 mT with simultaneous disappearance of the signal at ~330 mT. Finally, when 1 equiv. of Cu^{2+} was added to **1**, a signal corresponding to the second complex (with 1 : 1 ratio) could be detected clearer (with $A_{iso} = 5.4(1)$ mT and $g_{iso} = 2.127(1)$).

It is important to notice that even when more than 1 equiv. of Cu^{2+} was added, the only EPR signals recorded were those of the 1 : 1 complex and free Cu^{2+}. In fact, by subtracting the EPR signal of free Cu^{2+} from the spectra collected when more than 1 equiv. of Cu^{2+}

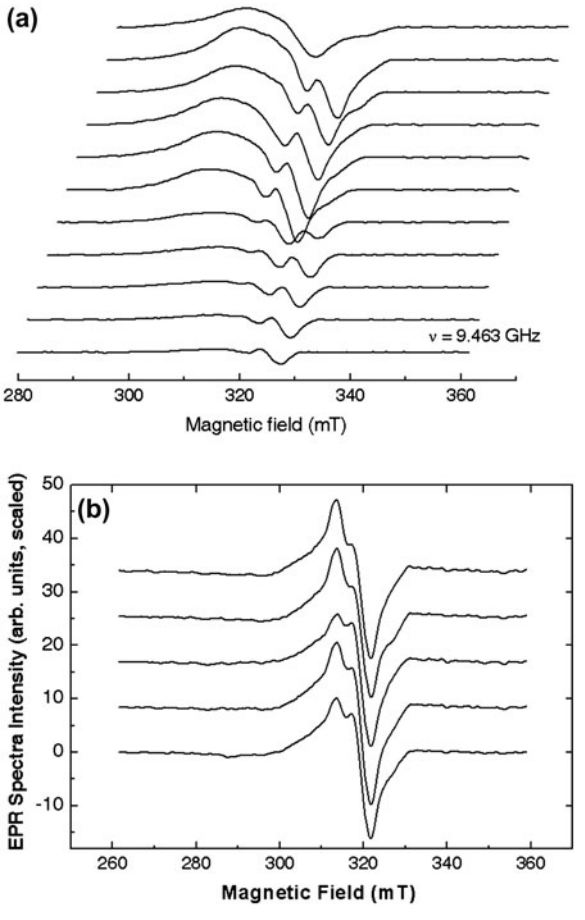

Figure 3. (a) From bottom to top: EPR titration measurements of **1** (2 mM) upon addition of increasing amounts of Cu^{2+} in ethanol (0.15, 0.30, 0.45, 0.60, 0.80, 1.00, 1.25, 1.50, 1.75, 2.00 equiv.). The top trace corresponds to free Cu^{2+} (2 mM) in ethanol; (b) from bottom to top: EPR titration measurements of **1** (2 mM) upon addition of increasing amounts of Cu^{2+} in ethanol (1.00, 1.25, 1.50, 1.75, 2.00 equiv.) after subtracting the signal of free Cu^{2+}.

was added, it can be seen that the signal of the 1 : 1 complex is constant (figure 3(b)). Therefore, it can be concluded that a 1 : 2 complex between **1** and Cu^{2+} was not detected by EPR measurements. However, the lack of observation of the 1 : 2 complex by the RT EPR experiments does not testify for its nonexistence. There could be several reasons for the inconsistency between the results of the EPR and other spectral techniques used, such as: (a) low abundance of the 1:2 complex could make it unobservable; (b) closeness of its EPR parameters (A_{iso}, *g*-factors) to those of the 1 : 1 complex could make these complexes indistinguishable; and c) non-zero probability of exchange interaction between the two Cu^{2+} cations of the 1 : 2 complex. This interaction may cause significant broadening of the Cu^{2+} EPR signals and/or formation of exchange dimer with large zero-field splitting parameters that also make this complex hardly detectable in the EPR spectra of solutions.

3.1.2. A proposed binding mechanism of 1 to Cu^{2+} in ethanol. Based on the above results of titration measurements, a step-by-step process is suggested (figure 4) where

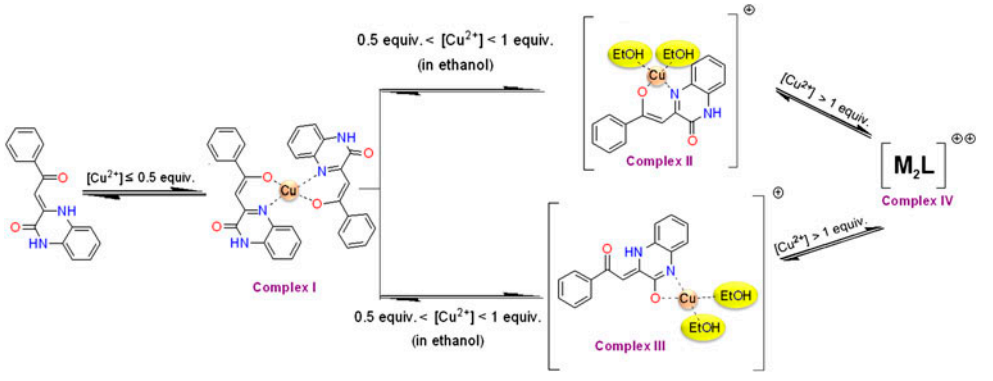

Figure 4. Suggested stepwise binding processes between Cu^{2+} and **1** (based on EPR, UV–vis and fluorescence titration measurements).

initially a 2 : 1 (ligand to metal) complex is formed (when no more than 0.5 equiv. of Cu^{2+} was added), followed by its conversion to two possible 1 : 1 complexes (II and III) at higher (0.5–1 equiv.) concentrations of Cu^{2+} and a 1 : 2 complex (IV) at Cu^{2+} above 1 equiv. The suggested mechanism is based on two assumptions: (a) the Cu^{2+} binding is accompanied by deprotonation of NH moiety for all the suggested complexes [23, 24]; (b) as in similar complexes reported in the literature [35–43] where favorable coordination of Cu^{2+} is 4 or 5, we have assumed that solvent molecules participate in the coordination to create chelates with square planar or square pyramidal geometries in complexes II and III, respectively. Five-coordinate copper complexes could be formed also in trigonal bipyramidal geometry [43]. Later (*vide infra*, Section 3.3.1) the results of geometry optimization calculations will show that complex III is not stable as a chelate, but as 'linear' through a Cu–N bond formation.

3.2. *Attempts to determine the actual binding site by using fragments of 1*

The observation (figure 4) that a 1 : 2 ligand to metal complex (IV) is formed indicates that there are two active sites in **1** for metal binding. Attempts to determine (e.g. by FTIR, see suppl. info., figure S1) the actual active site in the 1 : 1 complex has been unsuccessful. Therefore, in order to determine which of the two is more important and is the actual one to bind Cu^{2+} in the 1 : 1 complex, additional examination of the binding mechanism to Cu^{2+} was carried out by synthesizing fragments **2–4** (each contains only one of the suspected binding sites in **1**) (scheme 1).

3.2.1. Examining the binding ability of analogs 2–3 to Cu^{2+}

3.2.1.1. UV–vis measurements. A solution of free **2** in ethanol displays two strong bands at 247 nm ($\varepsilon = 6.0 \times 10^3\ M^{-1}cm^{-1}$) and 356 nm ($\varepsilon = 2.8 \times 10^4\ M^{-1}cm^{-1}$) in its absorbance spectra (figure 5). The spectra collected for **2** in the presence and absence of 100 equiv. of different metal ions (Co^{2+}, Mn^{2+}, Zn^{2+}, Ca^{2+}, Mg^{2+}, Ni^{2+}, and Ag^{+}) showed no significant change in its shape or location (see suppl. info., figure S2). On the other hand, the addition of Cu^{2+} resulted in a decrease in the intensity of the band at 356 nm accompanied with a

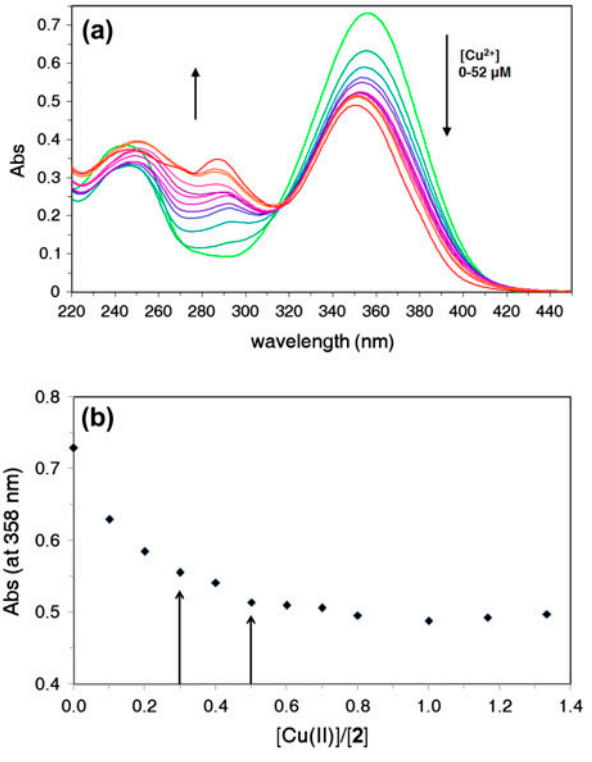

Figure 5. (a) UV–vis absorption spectral changes of **2** (24 µM) upon addition of increasing amounts of Cu^{2+} in ethanol (0, 2.4, 4.8, 7.2, 9.6, 12, 14.4, 16.8, 19.2, 28, 32, 36 µM). Arrows indicate the absorbences that increased (up) and decreased (down) during the titration experiments; (b) a plot of absorption of **2** in ethanol vs. the ratio of $[Cu^{2+}]/[\mathbf{2}]$ at 358 nm.

small blue shift (~5 nm) and an increase in the intensity of the bands at 247 and 290 nm (figure S2 and figure 5(a)). These observations indicate that **2** possess the ability to bind Cu^{2+} in ethanol. Binding of **2** to Cu^{2+} was reversible upon addition of EDTA (**2** and Cu^{2+} were regenerated).

The overlay of the UV–vis titration spectra indicates that the isosbestic point at ~320 nm was not conserved along the titration (figure 5(a)). The lack of a clear isosbestic point suggests that more than one type of complex is formed. Indeed the titration profile obtained from the absorbance of **2** with Cu^{2+} at 358 nm (figure 5(b)) shows at least two turning points in the plot when ~0.3 and 0.5 equiv. of Cu^{2+} were added, suggesting that respective 3 : 1 and 2 : 1 complexes are formed.

3.2.1.2. EPR measurements. EPR titration measurements of **2** with Cu^{2+} (figure 6) indicate that more than one type of complex is formed between **2** and Cu^{2+}. In fact, these measurements exhibit similar behavior to the EPR titration of the building block **1** (that includes both possible binding sites). As in the case of **1**, the EPR spectra collected during titration of **2** with Cu^{2+} clearly demonstrate that this fragment can coordinate to Cu^{2+} in a stepwise manner. Initially, when < 0.5 equiv. of Cu^{2+} was added, a 2 : 1 complex is predominant (with $A_{iso} = 6(0.5)$ mT and $g_{iso} = 2.112(5)$) and then, as the Cu^{2+} concentration increased, the initial signal was replaced by a new one, corresponding to a 1 : 1 complex

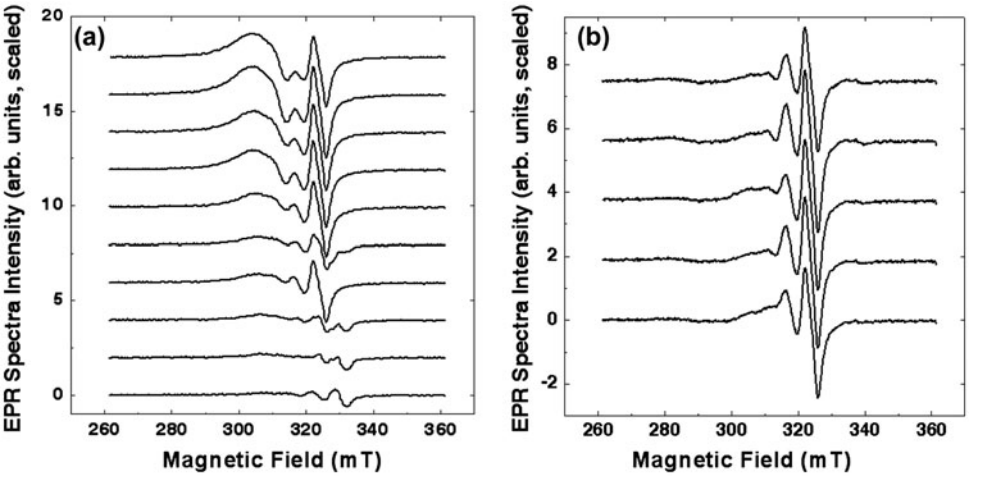

Figure 6. (a) From bottom to top: EPR titration measurements of **2** (2 mM) upon addition of increasing amounts of Cu^{2+} in ethanol (0.15, 0.30, 0.45, 0.60, 0.80, 1.00, 1.25, 1.50, 1.75, 2.00 equiv.); (b) from bottom to top: EPR titration measurements of **2** (2 mM) upon addition of increasing amounts of Cu^{2+} in ethanol (1.00, 1.25, 1.50, 1.75, 2.00 equiv.) after subtracting the signal of free Cu^{2+} ions in ethanol.

(with $A_{iso} = 6(0.5)$ mT and $g_{iso} = 2.143(5)$; see figure 6(a)). When more than 1 equiv. of Cu^{2+} was added, the signal remains constant with no indication of an additional complex being formed (figure 6(b)).

3.2.1.3. FTIR, HR-ESI-MS, and MALDI-TOF measurements. The FTIR spectrum is taken for the powder obtained from a mixture of **2** and 1 equiv. Cu^{2+} displays a significant change compared to the free ligand (see suppl. info., figure S3). The band at 1623 cm^{-1} that was assigned to the stretching vibration of the carbonyl in **2** disappeared. Also the N–H bending vibration at ~1545 cm^{-1} and the C–N and C–O stretching frequencies at 1284–1323 cm^{-1} disappeared as well. Furthermore, new absorptions at 1675 and 1712 cm^{-1} appeared. All these spectral changes indicate that a complex between Cu^{2+} and **2** was created.

Finally, a MALDI-TOF measurement of **2** and 1 equiv. of Cu^{2+} in ethanol : water was carried out. The result showed formation of a 1 : 1 complex with the appearance of intense mass at *m/z* 335.204 that corresponds to $[Cu(II)\ (\mathbf{2}\text{-}H)+2H_2O]^+$. The isotopic analysis of this peak also supports this observation. In addition, the detection of additional mass at *m/z* 353.205 suggests that $[Cu(II)\ (\mathbf{2}\text{-}H)+3H_2O]^+$ was formed as well (see suppl. info., figure S4).

Ligand **3** is similar to **2**, but more rigid. Its ability to bind Cu^{2+} was examined by FTIR spectroscopy (see suppl. info., figure S5) and the behavior was similar to that of **2**. In this case, the addition of Cu^{2+} to a solution of **3** in ethanol resulted instantly in precipitation of a greenish powder. The FTIR spectrum of this powder was significantly different from that obtained from free **3**. For instance, both the carbonyl stretch (1635 cm^{-1}) and the N–H bend (at 1571 cm^{-1}) found in the spectrum of free **3** disappeared in the greenish powder. New bands at 1328 and 1363 cm^{-1} appeared in the spectrum of **3** + 1 equiv. of Cu^{2+}. In addition, the N–H stretch at 3286 cm^{-1} disappeared while new bands at 438, 582, and 1610 cm^{-1} appeared, probably due to Cu–N, Cu–O and C = N vibrations, respectively [44–47]. Therefore, it seems that **3** also possess the ability to coordinate with Cu^{2+}.

3.2.2. Examining the binding ability of analogs 4 to Cu^{2+}

3.2.2.1. UV–vis, EPR, FTIR, and HR-ESI-MS measurements. The absorption spectra of ligand fragment **4** in ethanol displays a strong band at 250 nm ($\varepsilon = 1.5 \times 10^4$ $M^{-1}cm^{-1}$) and other bands that overlap with those of free Cu^{2+}. Indeed, when 100 equiv. of Cu^{2+} was added to **4** in ethanol, the only change observed was an increase in intensities of the bands. Hence, the binding of **4** and its ratio to Cu^{2+} could not be assessed from absorbance spectra. As a consequence, EPR titration was utilized to evaluate the binding ability and ratio between **4** and Cu^{2+}. During the titration, the only EPR signal that was recorded was that of free Cu^{2+} (with only minor splitting and change in the *g*-factor value that may indicate a weak interaction with Cu^{2+} (suppl. info., figure S5)). In addition, the FTIR spectrum of a powder obtained from a mixture of **4** with 1 equiv. of Cu^{2+} did not show any significant change that indicates complex formation. Only bands of both free perchlorate (624, 635, 1080, 1106, and 1140 cm^{-1}) [48] and **4** [49] were observed (see suppl. info., figure S6) with no indication of binding to Cu^{2+}. Also only ion masses of $[\mathbf{4}+H]^+$ and $[\mathbf{4}+Na]^+$ at *m/z* 148.07515 (calc. 148.07624) and 170.05708 (calc. 170.05819 *m/z*), respectively, were observed (see suppl. info., figures S7–S9).

Based on the above-described observations, whereas **2** and **3** exhibited the ability to bind to Cu^{2+} by different techniques, **4**, under similar conditions, did not show any evidence for its coordination with Cu^{2+}. Therefore, it is most probable that of the two binding sites in **1**, the one which exists in **2** and **3** (and not in **4**) is responsible to generate the 2 : 1 and 1 : 1 complexes I and II (figure 4).

3.3. *Computations*

3.3.1. Geometrical optimization. The lack of experimental evidence for the existence of complex III by spectral methods described above, as well as the lack of X-ray structures, prompted us to do comparative computations between complexes II and III to obtain their optimized geometries and at the same time, calculate various thermodynamic parameters (enthalpies, entropies, and Gibbs free energies) for the reactions of Cu^{2+} with **1** in ethanol.

Since the most common coordination numbers of Cu^{2+} are four and five [25], the first two entries in table 1 take into account a reaction between **1**, Cu^{2+}, and three molecules of ethanol. The results show that the values of ΔH and ΔG of II are more negative than those of III, indicating that the formation of II is more feasible thermodynamically than that of III by $\sim$12 kcal mol^{-1}. However, both reactions are exothermic.

The optimized geometries of **1** with Cu^{2+} and three molecules of ethanol afford geometrical structures of II and III, as shown in figure 7. In II, Cu^{2+} coordinates with nitrogen and oxygen of the ligand to form a six-membered chelate with bond lengths of 1.993 and

Table 1. Reaction entropies, enthalpies, and Gibbs free energies (ΔS in cal mol^{-1} K^{-1}, ΔH and ΔG in kcal mol^{-1}) for the reactions of Cu^{2+} and **1** in ethanol.

Reactions	ΔS	ΔH	ΔG
$Cu^{2+} + \mathbf{1} + 3C_2H_5OH \rightarrow$ Complex II	−67.38	−32.41	−12.32
$Cu^{2+} + \mathbf{1} + 3C_2H_5OH \rightarrow$ Complex III	−70.50	−21.70	−0.68
$Cu^{2+} + \mathbf{1} + 2C_2H_5OH \rightarrow$ Complex II	−31.40	−27.13	−17.76
$Cu^{2+} + \mathbf{1} + 2C_2H_5OH \rightarrow$ Complex III	−22.01	−18.78	−12.21

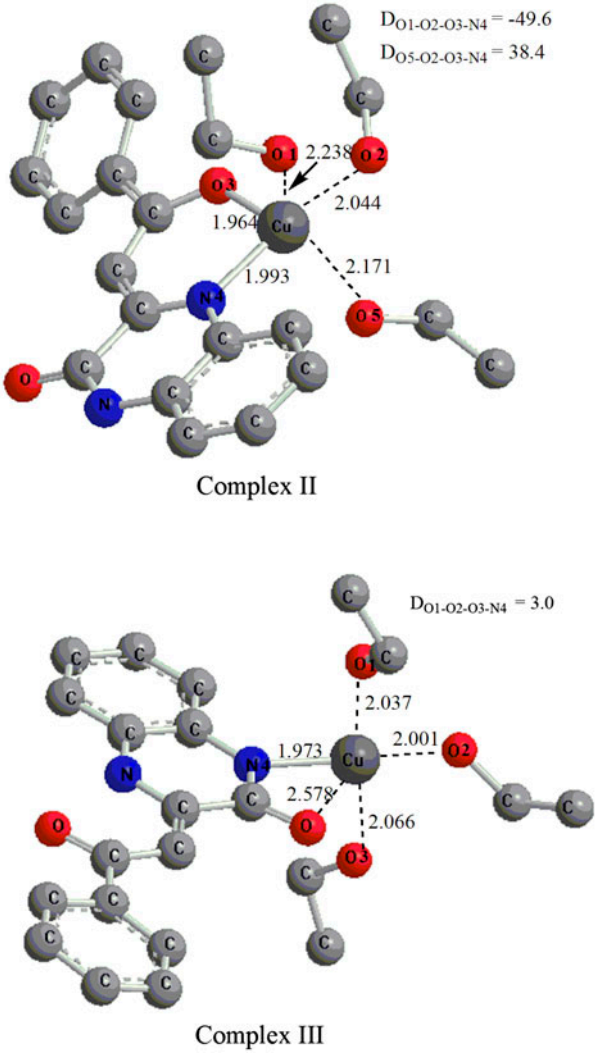

Figure 7. Optimized molecular structures of II and III (comprised of **1**, Cu^{2+} and three molecules of ethanol) by the density functional theory (DFT)-B3LYP level ('N' in blue, 'O' in red) (see http://dx.doi.org/10.1080/00958972.2013.803535 for color version).

1.964 Å for Cu–N and Cu–O, respectively. The coordination of Cu^{2+} with three molecules of ethanol affords two equatorial bond lengths of 2.044 Å and 2.171 Å and an axial bond of 2.238 Å. These bond lengths are comparable with other known and calculated copper complexes [38, 39, 50]. Complex II exhibits a distorted square pyramid structure with a dihedral angle of 38.4° involving the O5-O2-O3-N4 plane. On the other hand, III affords a non-chelated four-coordinate structure involving only nitrogen of ligand and three molecules of ethanol. The bond lengths are 1.973 Å for the Cu–N bond and 2.037, 2.001 and 2.066 Å for the three Cu–O bonds, respectively. The carbonyl oxygen of the ligand does not participate in coordination with the central Cu^{2+} because of the extreme Cu–O bond length of 2.578 Å. Also, the dihedral angle with the O5-O2-O3-N4 plane is 3°, indicating that III affords a square planar rather than tetrahedral geometry.

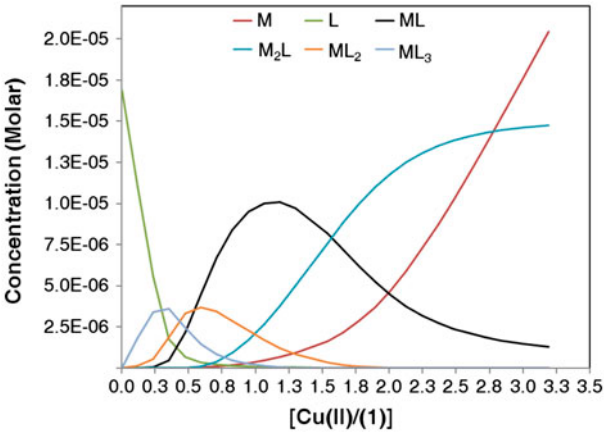

Figure 8. Concentration profiles calculated by using ReactLab™ Equilibrium program for free L = **1**, free M = Cu^{2+} and the four suggested complexes ML_3, ML_2, ML and M_2L in ethanol.

Table 2. Binding constants (log (β)) and Gibbs free energies of Cu(II) complexes with **1** in ethanol (298 K).

Reactions	log (β)	ΔG (kcal mol^{-1})
$ML_2 + L \leftrightarrow ML_3$	6.040 ± 0.030	−8.24 ± 0.55
$ML + L \leftrightarrow ML_2$	6.356 ± 0.017	−8.67 ± 0.57
$M + L \leftrightarrow ML$	8.452 ± 0.114	−11.53 ± 0.46
$ML + M \leftrightarrow M_2L$	5.752 ± 0.101	−7.85 ± 0.47

The results of calculations of **1**, Cu^{2+}, and two molecules of ethanol are shown in the last two entries of table 1. Also in this case, both reactions are exothermic and II is more stable than III. The optimized geometry of **1** with Cu^{2+} and two molecules of ethanol (figure S10) for II affords a distorted square-planar structure with a dihedral angle of 49.7° involving the O1-O2-O3-N4 plane. It forms a six-membered chelate ring with bond lengths of 1.988 and 1.963 Å for Cu–N and Cu–O, respectively. The central Cu^{2+} also coordinates with two molecules of ethanol with Cu–O bond lengths of 2.068 and 2.050 Å. Once again, a non-chelated structure is obtained for III (with a Cu–N bond of 1.961 Å; the Cu–O distance in this structure is 2.761 Å).

3.3.2. Stability constants and stoichiometries. We have found indications for formation of 2 : 1, 1 : 1, and 1 : 2 ligand to metal stoichiometries (figure 2), and 3 : 1 and 2 : 1 (figure 5(b)) when measurements were done 2 h after the addition of Cu^{2+}. Spectrophotometric data were also collected for **1** with Cu^{2+} at shorter times (minutes, figure S11). Conducting a spectral fitting (ReactLab™ Equilibrium program) for these data suggests that the formerly mentioned stoichiometries between **1** (and **2**) and Cu^{2+} could be formed at this relatively short time frame (figure 8).

The computed binding constants and their corresponding Gibbs free energies at 298 K for the four suggested complexes are presented in table 2. All calculated stability constants afford high values and although there is no clear trend, the results indicate that the 1 : 1 complex is most favored. The experimental ΔG value obtained here for the 1 : 1 complex

is comparable with that obtained above from the computation of a 1 : 1 complex (with three molecules of ethanol) (table 1).

4. Conclusions

Step-by-step binding processes take place between **1** and added Cu^{2+}. At first, when less than 0.5 equiv. of Cu^{2+} is added, the formation of 3 : 1 and 2 : 1 (**1**/Cu^{2+}) complexes predominate and upon addition of more Cu^{2+}, 1 : 1, and 1 : 2 complexes are favored. To understand whether the β-enaminoketone moiety or lactam moiety of **1** participates in coordination with Cu ion to form a 1 : 1 complex, density functional theory was used to optimize the geometries on the basis of the assumption that the common coordination number of Cu complex could be 4 or 5. The results of calculated optimized geometries indicate that the β-enaminoketone takes part in coordination of the favored 1 : 1 complex, either with two or three molecules of ethanol, to give four- and five-coordination, respectively. However, according to theoretical calculations, formation of a four-membered chelate structure with the lactam is disfavored. Computer simulation of the spectral data to extract stability constants of all discussed complexes also indicates that the 1 : 1 complex is most stable.

Among the fragments of **1**, derivatives **2** and **3** (with the β-enaminoketone moiety) exhibit similar behavior to **1**, while **4** (with the lactam) did not show any ability to bind Cu^{2+}. These findings indicate that the complexes being formed in the step-by-step mechanism (between **1** and Cu^{2+}) involves the β-enaminoketone moiety in **1** exclusively. Therefore, the lactam in **1** is not important for ligation of Cu^{2+} and could be replaced, for instance, by a carbon-based skeletal moiety.

Acknowledgments

This work was supported by grants from the National Basic Research Program of China (No. 2009CB930200), The National Key Technology R&D Program (2011BAD23B01), Beijing Natural Science Foundation (No. 7112008) and Beijing City Education Committee (KM201010005009). The authors are thankful to Dr Peter King and Prof. Marcel Maeder for their assistance with the data analysis using ReactLab™ Equilibria program and to Mrs. E. Solomon for technical assistance. JYB is grateful to (the late) Mrs. Irene Evens for supporting this research.

References

[1] J.F. Callan, A.P. de Silva, D.C. Magri. *Tetrahedron*, **61**, 8551 (2005).
[2] K.J. Wallace. *Supramol. Chem.*, **21**, 89 (2009).
[3] L. Prodi, F. Bolletta, M. Montalti, N. Zaccheroni. *Coord. Chem. Rev.*, **205**, 59 (2000).
[4] C. Bargossi, M.C. Fiorini, M. Montalti, L. Prodi, N. Zaccheroni. *Coord. Chem. Rev.*, **208**, 17 (2000).
[5] D.G. Barceloux. *Clin. Toxicol.*, **37**, 217 (1999).
[6] J.M. Matés, J.A. Segura, F.J. Alonso, J. Márquez. *Free Radical Biol. Med.*, **49**, 1328 (2010).
[7] Y.H. Hung, A.I. Bush, R. Alan. *J. Biol. Inorg. Chem.*, **15**, 61 (2010).
[8] T. Wang, Z. Guo. *Curr. Med. Chem.*, **13**, 525 (2006).
[9] N.K. Singhal, B. Ramanujam, V. Mariappanadar, C.P. Rao. *Org. Lett.*, **8**, 3525 (2006).
[10] G.S. Baghel, B. Ramanujam, C.P. Rao. *J. Photochem. Photobiol., A*, **202**, 172 (2009).
[11] X. Qi, E.J. Jun, L. Xu, S.-J. Kim, J.S.J. Hong, Y.J. Joon, J.Y. Yoon. *J. Org. Chem.*, **71**, 2881 (2006).

[12] Y. Zhou, F. Wang, Y. Kim, S.-J. Kim, J. Yoon. *Org. Lett.*, **11**, 4442 (2009).
[13] Y. Xiang, A. Tong, P. Jin, Y. Ju. *Org. Lett.*, **8**, 2863 (2006).
[14] K. Li, N. Li, X. Chen, A. Tong. *Anal. Chim. Acta*, **712**, 115 (2012).
[15] N. Narayanaswamy, T. Govindaraju. *Sens. Actuators, B*, **161**, 304 (2012).
[16] D. Maity, A.K. Manna, D. Karthigeyan, T.K. Kundu, S.K. Pati, T. Govindaraju. *Chem. Eur. J.*, **17**, 11152 (2011).
[17] S.Y. Lee, H.J. Kim, J.-S. Wu, K. No, J.S. Kim. *Tetrahedron Lett.*, **49**, 6141 (2008).
[18] H.S. Jung, P.S. Kwon, J.W. Lee, J.I. Kim, C.S. Hong, J.W. Kim, S. Yan, J.Y. Lee, J.H. Lee, T. Joo, J.S. Kim. *J. Am. Chem. Soc.*, **131**, 2008 (2009).
[19] L. Huang, F. Chen, P. Xi, G. Xie, Z. Li, Y. Shi, M. Xu, H. Liu, Z. Ma, D. Bai, Z. Zeng. *Dyes Pigm.*, **90**, 265 (2011).
[20] L. Huang, X. Wang, G. Xie, P. Xi, Z. Li, M. Xu, Y. Wu, D. Bai, Z. Zeng. *Dalton Trans.*, **39**, 7894 (2010).
[21] W. Wang, A. Fu, J. You, G. Gao, J. Lan, L. Chen. *Tetrahedron*, **66**, 3695 (2010).
[22] Y. Liu, Y. Sun, J. Du, X. Lv, Y. Zhao, M. Chen, P. Wang, W. Guo. *Org. Biomol. Chem.*, **9**, 432 (2011).
[23] E. Korin, B. Cohen, Y.-S. Xu, C.-C. Zeng, J.Y. Becker. *Tetrahedron*, **67**, 6252 (2011).
[24] E. Korin, B. Cohen, C.-C. Zeng, J.Y. Becker. *Tetrahedron*, **68**, 7450 (2012).
[25] A.D. Becke. *J. Chem. Phys.*, **98**, 5648 (1993).
[26] C.T. Lee, W.T. Yang, R.G. Parr. *Phys. Rev. B*, **37**, 785 (1988).
[27] J. Tomasi, M. Persico. *Chem. Rev.*, **94**, 2027 (1994).
[28] M.J. Frisch, G.W. Trucks, H.B. Schlegel, G.E. Scuseria, M.A. Robb, J.R. Cheeseman, J.A. Montgomery, Jr., T. Vreven, K.N. Kudin, J.C. Burant, J.M. Millam, S.S. Iyengar, J. Tomasi, V. Barone, B. Mennucci, M. Cossi, G. Scalmani, N. Rega, G.A. Petersson, H. Nakatsuji, M. Hada, M. Ehara, K. Toyota, R. Fukuda, J. Hasegawa, M. Ishida, T. Nakajima, Y. Honda, O. Kitao, H. Nakai, M. Klene, X. Li, J. E. Knox, H.P. Hratchian, J.B. Cross, V. Bakken, C. Adamo, J. Jaramillo, R. Gomperts, R.E. Stratmann, O. Yazyev, A.J. Austin, R. Cammi, C. Pomelli, J.W. Ochterski, P.Y. Ayala, K. Morokuma, G.A. Voth, P. Salvador, J.J. Dannenberg, V.G. Zakrzewski, S. Dapprich, A.D. Daniels, M.C. Strain, O. Farkas, D.K. Malick, A.D. Rabuck, K. Raghavachari, J.B. Foresman, J.V. Ortiz, Q. Cui, A.G. Baboul, S. Clifford, J. Cioslowski, B.B. Stefanov, G. Liu, A. Liashenko, P. Piskorz, I. Komaromi, R.L. Martin, D.J. Fox, T. Keith, M.A. Al-Laham, C.Y. Peng, A. Nanayakkara, M. Challacombe, P.M.W. Gill, B. Johnson, W. Chen, M.W. Wong, C. Gonzalez, J.A. Pople. *Gaussian 03, Revision C.02*, Gaussian, Wallingford, CT (2004).
[29] V. Sridharan, C. Avendano, J.C. Menendez. *Synlett*, **6**, 881 (2007).
[30] Z.-H. Zhang, L. Yin, Y.-M. Wang. *Adv. Synth. Catal.*, **348**, 184 (2006).
[31] Z.T. Huang, P.C. Zhang. *Chem. Ber.*, **122**, 2011 (1989).
[32] C.-X. Wu, L.-Y. Dai, Y.-Q. Chen, Z.-X. Weng. *Huaxue Tongbao.*, **66**, 337, [Abstract retrieved from Scifinder database (accession number 2003:482031)] (2003).
[33] W. Zhou, L.-R. Zhang, N. Jiao. *Tetrahedron*, **65**, 1982 (2009).
[34] N.J. Parmar, H.A. Barad, B.R. Pansuriya, R.A. Patel. *J. Coord. Chem.*, **64**, 688 (2011).
[35] A.K. Katz, Liat Shimoni-Livny, O. Navon, N. Navon, C.W. Bock, J.P. Glusker. *Helv. Chim. Acta*, **86**, 1320 (2003).
[36] M. Corsini, P. Zanello, R. Cini, G. Tamasi. *Acta Crystallogr., Sect. C: Cryst. Struct. Commun.*, **C65**, m219 (2009).
[37] Z.-L. You, Z.-D. Xiong, H.-L. Zhu. *Acta Crystallogr., Sect. E: Struct. Rep. Online*, **E60**, m1114 (2004).
[38] H.-N. Hou. *Acta Crystallogr., Sect. E: Struct. Rep. Online*, **E62**, m1940 (2006).
[39] T. Suksrichavalit, S. Prachayasittikul, C. Nantasenamat, C. Isarankurai-Na-Ayudhyal, V. Prachayasittikul. *Eur. J. Med. Chem.*, **44**, 3259 (2009).
[40] Y. Boukraa, T. Benabdallah. *J. Coord. Chem.*, **64**, 832 (2011).
[41] H.-H. Yao, W.-T. Huang, J.-M. Lo, F.-L. Liao, P. Chattopadhyay. *J. Coord. Chem.*, **58**, 975 (2005).
[42] Y.-F. Wang, Y.-M. Jiang, Z.-M. Liu, J.-M. Li. *J. Coord. Chem.*, **59**, 1977 (2006).
[43] B. Nath, D. Kalita, J.B. Baruah. *J. Coord. Chem.*, **64**, 2545 (2011).
[44] Y. Iwanami, T. Seki, T. Inagaki. *Bull. Chem. Soc. Jpn.*, **44**, 1316 (1971).
[45] Z. Chen, Y. Wu, D. Gu, F.I. Gan. *Dyes Pigm.*, **76**, 624 (2008).
[46] N.M. Hosny. *J. Mol. Struct.*, **923**, 98 (2009).
[47] T.M.A. Ismail. *J. Coord. Chem.*, **58**, 141 (2005).
[48] L.A. Saghatforoush, R. Mehdizadeh, F. Chalabian. *J. Chem. Pharm. Res.*, **3**, 691 (2011).
[49] W. Zhou, L. Zhang, N. Jiao. *Tetrahedron*, **65**, 1982 (2009).
[50] Y.X. Sun. *Acta Crystallogr., Sect. E: Struct. Rep. Online*, **E61**, m338 (2005).